

Luminescence of Ce³⁺ - and Eu²⁺ - doped silica glasses under UV and X-ray excitation

W. CHEWPRADITKUL^{a,*}, Y. SHEN^b, D. CHEN^b, M. NIKL^c, A. BEITLEROVA^c

^aDepartment of Physics, King Mongkut's University of Technology Thonburi, Bangkok 10140, Thailand

^bShanghai Institute of Optics and Fine Mechanics, CAS, Shanghai 201800, PR China

^cInstitute of Physics, AS CR, Cukrovarnicka 10, Prague 16253, Czech Republic

Ce³⁺- and Eu²⁺- doped silica glasses were prepared by impregnation of Ce and Eu ions, respectively, into porous silica glasses followed by high temperature sintering in a CO reducing atmosphere. The characteristic emission band of Ce³⁺ 5d → 4f transition peaking around 375 nm is observed in the luminescence spectra of Ce³⁺- doped glass under UV and X-ray excitation. Its photoluminescence decay is governed by several tens of nanoseconds decay time. For Eu²⁺- doped glass, the Eu²⁺ 5d → 4f emission band peaking around 430 nm is observed in the luminescence spectra and its photoluminescence decay is governed by a few microseconds decay time. The X-ray excited integral scintillation efficiency of about 82% and 120% of that of the Bi₄Ge₃O₁₂(BGO) crystal is obtained, respectively, for the Ce³⁺- and Eu²⁺- doped glasses. Scintillation light yield under gamma-ray excitation was also measured and compared with that of the BGO and CeF₃ crystals.

(Received February 7, 2013; accepted February 20, 2013)

Keywords: Ce³⁺, Eu²⁺, Luminescence, Photoluminescence decay, Porous materials, Scintillation

1. Introduction

Phosphors and scintillation materials have increasingly scientific and technological application in diverse fields. The search for appropriate phosphors and scintillation materials has been stimulated over a period of more than 100 years and a great number of materials have been found[1-3]. Rare-earth (RE) doping scintillating glass is an attractive material used in bulk or fiber forms for the detection of X-rays and nuclear radiation[4,5] as well as for applications in lighting and optical displays. They are cheaper and easier to fabricate with respect to single crystal materials, but they suffer from inefficient energy transfer and concentration quenching resulting in low light yield. Solubility of RE ions is low in silica glass prepared by direct high-temperature melting of RE compounds and raw materials of glass, and easily leads to segregation or clustering even at low concentration.

The Ce³⁺ and Tb³⁺ dopants are used most frequently in order to achieve fast (tens of ns) luminescence response in the blue spectral region and slow (units of ms) response in the green spectral region, respectively. Eu ion is studied both in trivalent and divalent charge state [6] and especially the latter appears to be interesting for obtaining of a broad-band emission in the blue-green spectral range with still reasonably fast decay times of hundreds of nanoseconds - few microseconds range. Several groups have addressed themselves to the problem of stabilization of 2⁺ charge state of Eu center in an oxide glass host [7-9].

In order to suppress concentration quenching of emission ions to obtain intense luminescence glass, our group have developed a novel method for uniform distribution of RE or transition metal ions in high silica

glass host [10,11]. In contrast to the direct introduction of RE ions into silica glasses by high-temperature melting, a three-step process was employed including preparation of a porous silica glass, adsorption of RE ions and high-temperature sintering in a reducing atmosphere. Very intense photoluminescence emissions were observed in the leached, sintered high silica glasses impregnated with Cu, Sn and Eu ions under UV excitation[11]. It confirmed the success in solving the mentioned problem of concentration quenching and segregation of emission centers based on the doped ions.

In this paper, we prepared Ce³⁺- and Eu²⁺-doped silica glasses by impregnation of Ce and Eu ions into porous silica glasses followed by high-temperature sintering in a CO reducing atmosphere and investigated their luminescence characteristics under UV and X-ray excitation. In order to evaluate the potential in scintillation applications, the integral scintillation efficiency and scintillation light yield (LY) of these glasses were also determined.

2. Experimental details

The porous glass was obtained by leaching the alkali-borate phase from phase - separated alkali - borosilicate glass in hot acid solution [10,11]. Reagent-grade chemicals SiO₂, H₃BO₃, Na₂CO₃, CaCO₃, and Al(OH)₃ were used as starting materials to produce an initial glass. The initial glass with the composition (in wt %) 51.8SiO₂ · 33.3B₂O₃ · 2.6Al₂O₃ · 4.0CaO · 8.3Na₂O was melted in a platinum crucible at 1400 °C for 4 h. The melt was then poured onto a preheated stainless steel plate and pressed to a thickness of about 2 mm by another plate. Phase separation of alkali-borate and silicate phases was

performed at 630 °C for 40 h. The obtained phase-separated glass was cut to pieces and polished with dimension of about 8×8×1 mm³, followed by leaching in hot (90°C) 1N HNO₃ solution for 48 h to remove alkaliborate phase. After washing with distilled water and drying, then leached porous glasses were obtained. The obtained porous glass contains over 96% of SiO₂ [10,11]. The pores smaller than 12 nm were distributed uniformly in the silica network and occupied about 40% volume of glass. Some porous glass samples were immersed in the 0.03 M solution of Ce(NO₃)₃ · 6H₂O and some samples were immersed in the 0.03 M solution of Eu(NO₃)₃ · 6H₂O for 1 h and dried at room temperature (RT). The porous glasses impregnated with Ce and Eu ions were then sintered at 1150°C for 2 h in a CO reducing atmosphere. The obtained glasses were compact, colorless and transparent with the density of 2.2 g/cm³ determined by Archimedes method. The polished plates of about 8×8×1 mm³ were used for all the measurements.

Excitation and emission spectra in the UV/visible region were recorded on a Hitachi F-2500 fluorescence spectrophotometer equipped with a 150 W xenon lamp source. Radioluminescence (RL) spectra and photoluminescence (PL) decay curves were obtained using the custom made 5000M fluorometer (Horiba Jobin Yvon) equipped with TBX-04 photon counting detector (IBH, UK), for details see Ref.[12]. A hydrogen-filled (ns pulsed) coaxial flashlamp was used for the PL decay measurements using the time-correlated single photon counting technique. An X-ray tube (Mo anode, 40 kV, 15 mA) was used for RL spectra measurements. RL spectra were corrected for experimental distortions. Convolution procedures (Spectra-Solve software package from Ames Photonics Inc.) were used to extract true decay times in the situation where the decay curves were distorted due to a finite width of the instrumental response. The integral scintillation efficiency of the glass samples was measured and compared to a comparable size Bi₄Ge₃O₁₂(BGO) reference scintillator.

LY measurements were performed by measuring scintillation pulse height spectra of 662 keV γ -rays from a ¹³⁷Cs source. The sample was coupled by silicone grease to the Photonis XP5200B photomultiplier tube (PMT) and covered with several layers of Teflon tape in a configuration of a reflective umbrella for better light collection. The signal from the PMT anode was processed by a Canberra 2005 preamplifier, a Tennelec TC243 spectroscopy amplifier with a shaping time of 4 μ s, and a multichannel analyzer (Tukan 8k). The LY, expressed as the number of photons per MeV of absorbed gamma energy, was measured for the glass samples and compared with BGO and CeF₃ scintillators. All the measurements were carried out at RT.

3. Results and discussion

3.1. Photoluminescence of Ce³⁺- doped silica glass

Fig. 1 presents the excitation (curves a, λ_{em} = 380 nm) and emission (curve b, λ_{ex} = 295 nm) spectra at RT for the Ce-doped silica glass (Ce-glass) sintered in a CO reducing

atmosphere. In the excitation spectrum, a broad band peaking at approximately 300 nm can be attributed to the absorption due to the 4f \rightarrow 5d transitions of Ce³⁺ ions. Characteristic broad band emission of Ce³⁺ is peaked around 380 nm under 295 nm excitation, but it is worth to note that the band is inhomogeneously broadened. This is rather typical situation of Ce³⁺ center in glassy environment, in which the change in the short distance order and eventual defects nearby will shift position of 5d₁ level and/ or change its relaxation pathway. Usually, the emission of Ce³⁺ ions occurs as a doublet band due to transitions from the relaxed lowest 5d excited state to the spin-orbit split 4f ground states (²F_{5/2}, ²F_{7/2}). At RT, these two bands merge into an asymmetric broad band because of the large spatial extension of the 5d wave function and its interaction with lattice vibrations.

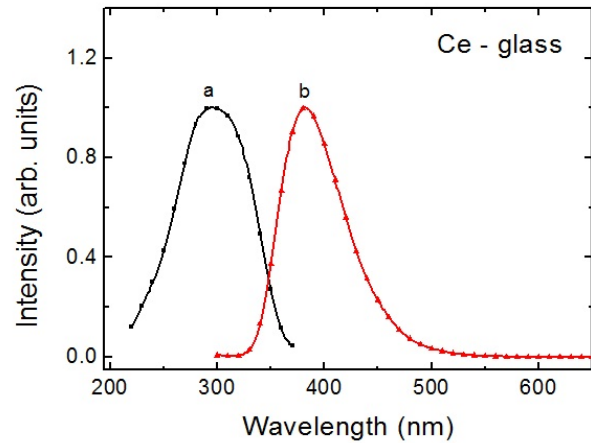


Fig. 1. Excitation (λ_{em} = 380 nm, curve a) and emission (λ_{ex} = 295 nm, curve b) spectra of Ce - glass as measured at RT.

The PL decay curves of the Ce-glass were measured at RT and are shown in Fig. 2. Each decay curve can be well fitted with a double – exponential equation, $I(t) = \sum A_i \exp(-t/\tau_i) + \text{background}$, $i = 1, 2$, where $I(t)$ is the luminescence intensity, A stands for the amplitude, t for the time and τ for the decay time constant of the exponential component. The PL decay at 370 nm under excitation at 290 nm (Fig.2a) yields the decay times $\tau_1 = 49$ ns and $\tau_2 = 177$ ns with respective component intensities $I_i = (A_i \tau_i) / (\sum A_i \tau_i)$, namely, $I_1 = 94.9\%$ and $I_2 = 5.1\%$, respectively. The PL decay at longer wavelength of 440 nm under excitation with 320 nm (Fig.2b) yields the decay times $\tau_1 = 56$ ns and $\tau_2 = 146$ ns with component intensities $I_1 = 80.7\%$ and $I_2 = 19.3\%$, respectively. The τ_1 decay times are typical for the 5d \rightarrow 4f radiative transition of Ce³⁺[13]. Increasing decay time value at longer emission wavelength is consistent with the above mentioned inhomogeneous broadening of Ce³⁺ emission band, indicating the presence of non-equivalent Ce³⁺ centers.

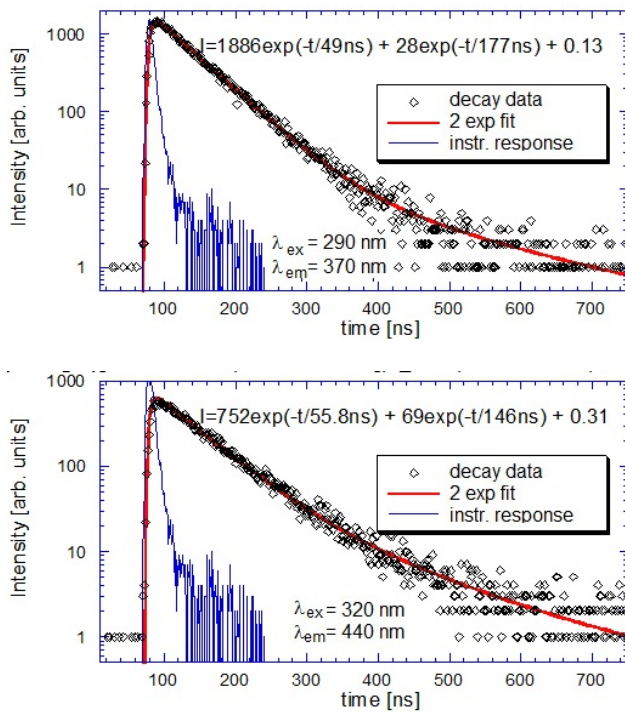


Fig. 2. PL decay curves of the Ce-glass as measured at RT [(a) $\lambda_{ex} = 290$ nm, $\lambda_{em} = 370$ nm ; (b) $\lambda_{ex} = 320$ nm, $\lambda_{em} = 440$ nm]. The solid lines are the convolution of the instrumental response and the function $I(t)$ given in the figures.

3.2. Photoluminescence of Eu^{2+} -doped silica glass

Fig. 3 presents the excitation (curves a, $\lambda_{em} = 434$ nm) and emission (curve b, $\lambda_{ex} = 282$ nm) spectra at RT for the Eu-doped silica glass (Eu-glass). In the excitation spectrum, a broad band from 230 up to 400 nm is observed with center at approximately 300 nm. It should be associated with the $4f^7[{}^8S_{7/2}] \rightarrow 4f^65d^1$ absorption transitions of Eu^{2+} ions in glassy environment, in which an asymmetric site yielding a large spatial extension of the 5d wave function. In the emission spectrum, a broad band associated with the $4f^65d^1 \rightarrow 4f^7[{}^8S_{7/2}]$ transition of the Eu^{2+} ions peaking around 434 nm dominates the spectrum and the emission lines within 590 - 620 nm due to the Eu^{3+} intraconfigurational emission transitions (${}^5D_0 \rightarrow {}^7F_{1,2}$) are absent. It indicates that Eu^{3+} ions efficiently transform into Eu^{2+} ions under high temperature (1150°C) sintering in a CO reducing atmosphere.

PL decays of the Eu-glass at RT are shown in Fig. 4. PL decay at 430 nm under excitation at 330 nm (Fig. 4a) yields the decay times $\tau_1 = 1.05$ μs and $\tau_2 = 1.95$ μs with component intensities $I_1 = 83\%$ and $I_2 = 17\%$, respectively. The PL decay at longer wavelength of 490 nm under excitation at 360 nm (Fig. 4b) yields the decay times $\tau_1 = 1.65$ μs and $\tau_2 = 4.27$ μs with component intensities $I_1 = 79\%$ and $I_2 = 21\%$, respectively. Such decay time values (τ_1) of a few microsecond [13] are typical for the $5d \rightarrow 4f$ radiative transition of Eu^{2+} . Depending on the excitation/emission wavelength combination and similarly to the Ce-glass, the low energy shift of excitation and

emission wavelength results in the slow-down of the decay.

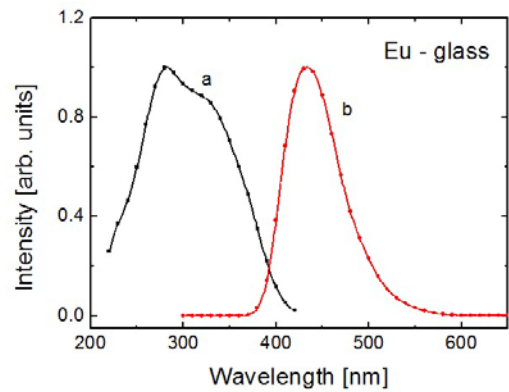


Fig. 3. Excitation ($\lambda_{em} = 434$ nm, curve a) and emission ($\lambda_{ex} = 282$ nm, curve b) spectra of Eu-glass as measured at RT.

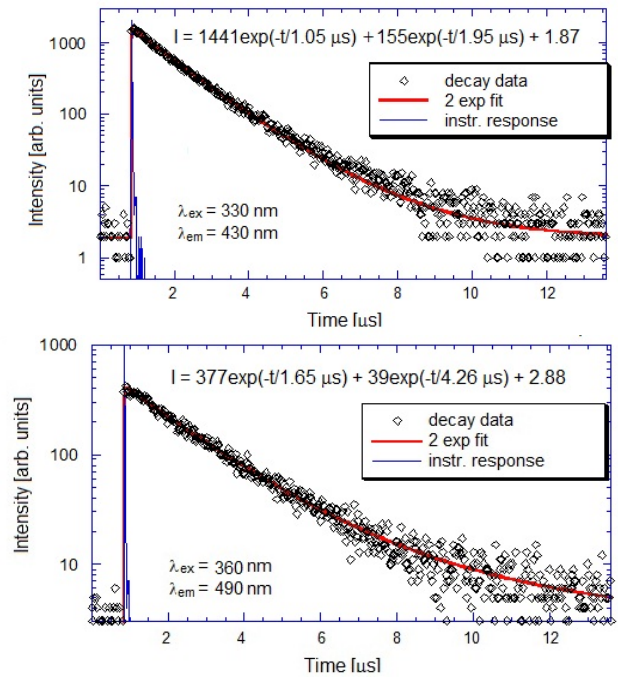


Fig. 4. PL decay curves of the Eu-glass as measured at RT [(a) $\lambda_{ex} = 330$ nm, $\lambda_{em} = 430$ nm ; (b) $\lambda_{ex} = 360$ nm, $\lambda_{em} = 490$ nm]. The solid lines are the convolution of the instrumental response and the function $I(t)$ given in the figures.

Somewhat non-exponential decays of Ce^{3+} and Eu^{2+} centers, and varying τ_1 values with emission wavelength are worth a comment. Similar phenomena can be noticed in the Ce^{3+} -doped oxide glass with high Gd_2O_3 content [14] and Ce^{3+} -doped silica glass [15,16]. The 5d wave function of both Ce^{3+} and Eu^{2+} excited states has a large extent due to crystal field strength at a given site of glass host. The dopant is embedded at a number of slightly non-equivalent sites in the glass matrix, the emission band broadens inhomogeneously and the decay time value varies as well. Nevertheless, the decay non-exponentiality

is rather small which means that the inhomogeneity of the Ce^{3+} and Eu^{2+} sites is rather small.

3.3 Radioluminescence of Ce^{3+} - and Eu^{2+} - doped silica glasses

RL spectra of Ce- and Eu- glasses and a BGO reference crystal recorded at RT are shown in Fig.5. The Ce-glass sample shows a broad emission band peaking around 375 nm due to the $5d \rightarrow 4f$ transitions of Ce^{3+} . The Eu-glass sample shows a broad emission band peaking around 430 nm due to the $5d \rightarrow 4f$ transitions of Eu^{2+} . Apparently, all these RL characteristics of Ce- and Eu- glasses are in line with the PL characteristics under UV excitation. This results further confirm rather small inhomogeneity of the Ce^{3+} and Eu^{2+} sites in the glass matrices. The glass samples and BGO sample are about the same size and the measurements were performed under the same experimental conditions, so that the spectra can be compared in an absolute way. The integral scintillation efficiency (integral of RL spectra) of the glass samples was determined from the ratio of the integrated intensity of RL spectra of the glass samples with that of the BGO reference sample. We obtained integral scintillation efficiency of about 82% and 120% of that of the BGO crystal for Ce- and Eu- glasses, respectively.

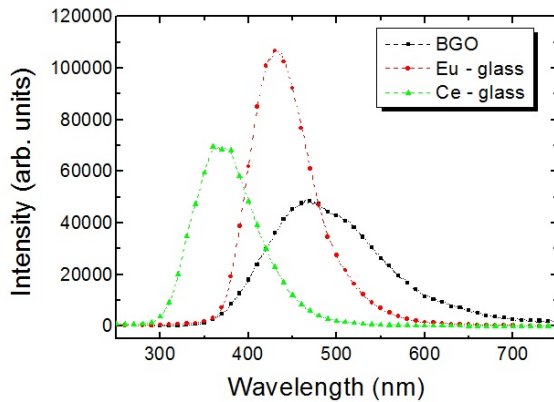


Fig. 5. RL spectra (X-ray irradiation: 40 kV, 15 mA) of Ce- and Eu- glasses and BGO crystal at RT. The spectra are mutually comparable in an absolute way.

3.4. Light yield of Ce^{3+} - and Eu^{2+} - doped silica glasses

Fig.6 presents the scintillation pulse height spectra of 662 keV γ -rays from a ^{137}Cs source as measured with glass samples, CeF_3 and BGO crystals, but with lower amplification gain factor of 0.18 for BGO. The intensity of a scintillation pulse (x-axis), expressed as a number of photoelectrons released by the PMT photocathode in a scintillation event, was obtained by relating the position of the ^{137}Cs 662 keV full energy peak in pulse height spectra of the BGO or CeF_3 crystals with that of the position corresponding to the single photoelectron peak from the

PMT photocathode [17,18]. We obtained photoelectron yield of 1850 and 260 photoelectrons per MeV (phe/MeV) for BGO and CeF_3 crystals, respectively. By taking into account the quantum efficiency (QE) of the PMT for BGO (21% at peak emission 480 nm) and CeF_3 (6% at peak emission 290 nm), we estimated the LY of 8810 and 4330 photons/MeV (ph/MeV), respectively, for BGO and CeF_3 crystals. Unfortunately, the glass samples show only the Compton continuum (CC) with the absence of 662 keV full energy peak in the pulse height spectra. This is due to low density and effective atomic number of the glass matrix. However, we can estimate the LY of the glass samples using the position of Compton edge (CE), which corresponds to a maximum energy of Compton electron ($E_e = 477$ keV), in the pulse height spectrum of 662 keV γ -rays. It must be noted that exact position of CE in the CC is not located at the same position with Compton maximum (CM) but it slightly shifts to higher energy shoulder [19]. A rough estimate of the CE position for a low density glass scintillator can be obtained by assuming a fraction of 0.8 of CM [19] at which CE crosses the CC spectrum (see Fig.6).

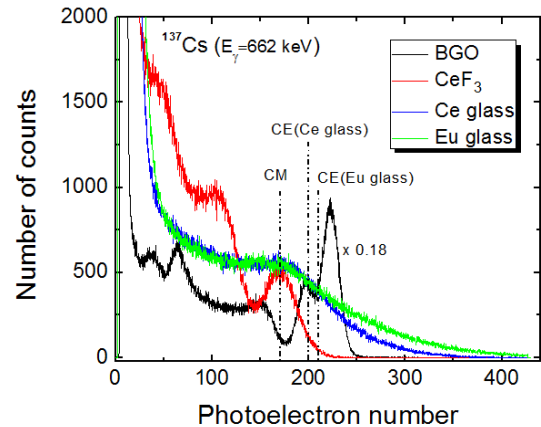


Fig. 6. Pulse height spectra of 662 keV γ -rays from a ^{137}Cs source as measured with Ce-, Eu- glasses, CeF_3 and BGO (with a lower gain factor of 0.18) crystals.

We estimated photoelectron yield of 420 and 440 phe/MeV (at $E_e = 477$ keV) for Ce- and Eu- glasses, respectively. By taking into account the QE of the PMT for Ce-glass (30% at peak emission 375 nm) and Eu-glass (29% at peak emission 430 nm), these values correspond to the LY of 1400 and 1520 ph/MeV, respectively, for Ce- and Eu-glasses. In spite of comparable integral scintillation efficiency under X-ray irradiation ($E_x \leq 40$ keV), the LY of the glass samples under excitation with high energy (662 keV) γ -rays is much lower i.e. about 16-17% of that of BGO crystal (as measured at shaping time of 4 μs). This indicates to a strong slow-down effect in the transport stage of scintillation process in scintillating glasses. Taken together, this effect and short-range order of glass matrix demonstrate that the energy transfer efficiency of scintillating glasses is much lower with respect to single crystal materials, thus reducing their LY.

The results summarizing photoelectron yield and LY measured at 662 keV γ - rays are presented in Table 1.

Table 1. Photoelectron yield and LY of Ce- and Eu- glasses, CeF_3 and BGO crystals.

Scintillator	Photoelectron yield [phe/MeV]	Light yield [ph/MeV]
BGO	1850 \pm 90	8810 \pm 880
CeF_3	260 \pm 10	4330 \pm 430
Ce-glass	420 \pm 20	1400 \pm 140
Eu-glass	440 \pm 20	1520 \pm 150

4. Conclusions

The Ce^{3+} - and Eu^{2+} - doped silica glasses with small inhomogeneity of Ce and Eu sites were successfully prepared as intense luminescence materials by impregnation of $Ce(NO_3)_3$ and $Eu(NO_3)_3$ solutions into porous silica glasses and sintered at 1150°C in a CO reducing atmosphere. The Ce- glass exhibits an intense violet-blue emission of Ce^{3+} ions under UV excitation with dominating fast decay time of about 50 ns. The Eu- glass exhibits an intense blue emission of Eu^{2+} ions under UV excitation with somewhat longer decay time value of about 1 μ s. The Eu- glass has integral scintillation efficiency of about 120% of that of the BGO crystal, which is significantly higher than that of about 82% of that of the BGO crystal obtained for the Ce- glass. It seems worthwhile to further enhance the scintillation efficiency of Ce- and Eu- glasses e.g. by introducing the Gd^{3+} energy guiding sublattice studied in phosphate glasses and by Ce^{3+} / Eu^{2+} codoping, which provides an efficient energy transfer by resonance processes from Gd^{3+} to Ce^{3+} and from Ce^{3+} to Eu^{2+} . Both glasses can be excited efficiently using UV lamps and X-rays and could be also used as phosphors for developing new UV and X-ray sensors.

Acknowledgements

The authors acknowledge valuable contribution from KMUTT graduate student Chalerm Wanarak. This work is financially supported by the NRCT-NSFC project (NSFC Nos.60878043 and 50911140475), the TICA-MOST project (No.19-502J) and the National Research University Project of Thailand's Office of the Higher Education Commission. Partial support of Czech MSMT KONTAKT II grant LH12185 is also gratefully acknowledged.

References

- [1] M. J. Weber, *J. Lumin.* **100**, 35(2002).
 [2] M. Nikl, *Meas. Sci. Technol.* **17**, R37 (2006).

- [3] C. Ronda, *Luminescence : From Theory to Applications*, Wiley-Vch Verlag GmbH&Co. KGaA, Weinheim, 2008.
 [4] G. Zanella, R. Zannoni, R. Dall'Igna, P. Polato, M. Bettinelli, *Nucl. Instrum. Methods Phys. Res. A* **359**, 547 (1995).
 [5] M. Nikl, K. Nitsch, E. Mihokova, N. Solovieva, J.A. Mares, P. Fabeni, G.P. Pazzi, M. Martini, A. Vedda, S. Baccaro, *Appl. Phys. Lett.* **77**, 2159 (2000).
 [6] J. A. Sampaio et al., *J. Phys.: Condens. Matter* **22**, 055601 (2010).
 [7] E. Malchukova, B. Boizot, *Mater. Res. Bull.* **45**, 1299 (2010).
 [8] Q. Zhang, X. Liu, Y. Qiao, B. Qian, G. Dong, J. Ruan, Q. Zhou, J. Qiu, D. Chen, *Opt. Mater.* **32**, 427 (2010).
 [9] S. Liu, G. Zhao, W. Ruan, Z. Yao, T. Xie, J. Jin, H. Ying, J. Wang, G.Han, *J. Am. Ceram. Soc.* **91**, 2740 (2008).
 [10] J. Xia, D. Chen, J. Qiu, C. Zhu, *Opt. Lett.* **30**, 47 (2005).
 [11] D. Chen, H. Miyoshi, T. Akai, T. Yazawa, *Appl. Phys. Lett.* **86**, 231908 (2005).
 [12] H. Feng, V. Jary, E. Mihokova, D. Ding, M. Nikl, G. Ren, H. Li, S. Pan, A. Beitlerova, R. Kucerkova, *J. Appl. Phys.* **108**, 033519 (2010).
 [13] G. Blasse, B.C. Grabmaier, *Luminescent Materials*, Springer, Berlin, 46(1994).
 [14] W. Chewpraditkul, X. He, D. Chen, Y. Shen, Q. Zhang, B. Yu, M. Nikl, R. Kucerkova, A. Beitlerova, C. Wanarak, A. Phunpueok, *Phys. Status Solidi A* **208**, 2830 (2011).
 [15] A. Vedda, N. Chiodini, D. Di Martino, M. Fasoli, S. Keffer, A. Lauria, M. Martini, F. Moretti, G. Spinolo, M. Nikl, N. Solovieva, G. Brambilla, *Appl. Phys. Lett.* **85**, 6356 (2004).
 [16] A. Vedda, N. Chiodini, D. Di Martino, M. Fasoli, F. Morazzoni, F. Moretti, R. Scotti, G. Spinolo, A. Baraldi, R. Capelletti, M. Mazzera, M. Nikl, *Chem. Mater.* **18**, 6178 (2006).
 [17] M. Moszynski, M. Kapusta, M. Mayhugh, D. Wolski, S.O. Flyckt, *IEEE Trans. Nucl. Sci.*, **44**, 1052 (1997).
 [18] M. Bertolaccini, S. Cova, C. Bussolatti, A technique for absolute measurement of the effective photoelectron per keV yield in scintillation counters, in *Proc. Nuclear Electronics Symp., Versailles, France*, (1968).
 [19] L. Swiderski, M. Moszynski, W. Czarnacki, J. Iwanowska, A. Syntfeld-Kazuch, T. Szczesniak, G. Pausch, C. Plettner, K. Roemer, *Rad. Meas.* **45**, 605 (2011).

*Corresponding authors: weerapong.che@kmutt.ac.th